

Are your MRI contrast agents cost-effective?

Learn more about generic Gadolinium-Based Contrast Agents.



AJNR

**New Morphologic Variants of the Hand
Motor Cortex as Seen with MR Imaging in a
Large Study Population**

M. Caulo, C. Briganti, P.A. Mattei, B. Perfetti, A. Ferretti,
G.L. Romani, A. Tartaro and C. Colosimo

This information is current as
of April 20, 2024.

AJNR Am J Neuroradiol 2007, 28 (8) 1480-1485

doi: <https://doi.org/10.3174/ajnr.A0597>

<http://www.ajnr.org/content/28/8/1480>

ORIGINAL
RESEARCH

M. Caulo
C. Briganti
P.A. Mattei
B. Perfetti
A. Ferretti
G.L. Romani
A. Tartaro
C. Colosimo

New Morphologic Variants of the Hand Motor Cortex as Seen with MR Imaging in a Large Study Population

BACKGROUND AND PURPOSE: The hand motor cortex (HMC) has been classically described as having an omega or epsilon shape in axial-plane images obtained with CT and MR imaging. The aim of this study was to use MR imaging and Talairach normalization in a large sample population that was homogeneous for age and handedness to evaluate in a sex model a new classification with 5 morphologic variants of the HMC in the axial plane (omega, medially asymmetric epsilon, epsilon, laterally asymmetric epsilon, and null).

MATERIALS AND METHODS: Structural brain MR images were obtained from 257 right-handed healthy subjects (143 men and 114 women; mean age, 23.1 ± 1.1 years) via a Talairach space transformed 3D magnetization-prepared rapid acquisition of gradient echo sequence. The frequencies of the different HMC variants were reported for hemisphere and sex.

RESULTS: The new variants of the HMC (medially asymmetric epsilon, laterally asymmetric epsilon, and null) were observed in 2.9%, 7.0%, and 1.8% of the hemispheres, respectively. Statistically significant sex differences were observed: The epsilon variant was twice as frequent in men, and an interhemispheric concordance for morphologic variants was observed only for women.

CONCLUSION: The large study population permitted the description of a new morphologic classification that included 3 new variants of the HMC. This new morphologic classification should facilitate the identification of the precentral gyrus in subsequent studies and in everyday practice.

MR imaging allows a noninvasive study of the morphology of the cortical surface of the brain with a high degree of spatial resolution. The cortical anatomy of cerebral gyri is complex and presents tremendous intra- and intersubject variability. Therefore, the identification of specific cortical regions based only on morphologic features can be challenging. The presence of space-occupying lesions in the brain, such as tumors or vascular malformations, can further complicate this procedure by distorting normal anatomy, thereby making the identification of specific cortical regions difficult or impossible.

With the development of the concept of “homunculus,” the cortical representation of motor hand function is known to be located in the superior aspect of the precentral gyrus.¹⁻³ Even though functional techniques have recently permitted the identification of anatomic regions based on the correspondence with regions of activation,^{4,5} the knowledge of pure anatomic landmarks of the cerebral cortex remains of fundamental importance in research and everyday clinical practice. In fact, functional imaging is not widely available and requires extra time for data acquisition/analysis and a high-field MR imaging unit equipped with strong and rapid gradients.

Several authors have studied the radiologic anatomy of the

central region,⁶⁻⁹ applying different methods based on various morphologic features to localize the precentral gyrus.¹⁰⁻¹² Previous articles described the hand motor cortex (HMC) in dissected brains or on CT or MR imaging as having either the shape of a typical hook,¹³ bayonet, step, or zigzag on the sagittal plane.¹⁴ Other authors¹⁵ described this structure as a knuckle or as a structure like an omega on the axial plane.¹⁶ Yousry et al¹⁷ defined the “omega” as the most reliable landmark for the identification of the precentral gyrus. The characteristic inverted omega (Ω) shape of the HMC in the axial plane was explained by the presence of 2 anteriorly directed small fissures, which stem from the middle genu of the precentral sulcus. Occasionally, the presence of a third fissure, placed between the first 2, confers a characteristic horizontal epsilon (ϵ) shape.¹⁷ They also localized blood oxygen level-dependent (BOLD) functional MR imaging (fMRI) activation, obtained during hand movement exactly on the omega region of the precentral gyrus. The cortical representation of hand motor function was, therefore, localized in the precentral gyrus and characterized as having either an inverted omega shape or, sometimes, a horizontal epsilon shape in axial scans, whereas it assumed the shape of a posteriorly directed hook in the sagittal plane.¹⁷

Our clinical and research experience in MR imaging studies suggested that the different shapes that the HMC can assume in the axial plane are more varied than the 2 classic types previously described. Specifically, we postulated that the classic epsilon morphologic variant could be further subdivided into 3 forms: medially asymmetric epsilon, epsilon, and laterally asymmetric epsilon. We also included the null variant that, although previously reported, has not, to our knowledge, been adequately described and classified.

Sex-related differences in the complexity of sulcal and gyral arrangement of the cerebral cortex have been reported.¹⁸ Sim-

Received November 2, 2006; accepted after revision January 25, 2007.

From the Institute Advanced Biomedical Technologies of the Department of Clinical Sciences and Bioimaging (M.C., C.B., P.A.M., B.P., A.F., G.L.R., A.T.), University “G. d’Annunzio,” Chieti, Italy; and the Department of Radiology (C.C.), Catholic University of Rome, Italy.

This work was supported in part by a grant from the Italian Ministry of Research to the Center of Excellence on Aging of the University “G. d’Annunzio” of Chieti-Pescara.

Paper previously presented in part at: Annual Meeting of the American Society of Neuroradiology, May 3, 2006; San Diego, Calif.

Please address correspondence to Massimo Caulo, MD, PhD, ITAB—Institute for Advanced Biomedical Technologies, University “G. d’Annunzio” of Chieti-Pescara, Via dei Vestini, n. 33, 66100 Chieti, Italy; e-mail: massimo.caulo@itab.unich.it

DOI 10.3174/ajnr.A0597

ilar results have not been reported for handedness, but morphometric variations have been described.^{19,20}

The aim of this study was to use MR imaging and Talairach normalization in a large sample population that was homogeneous for age and handedness to evaluate in a sex model a new classification of the morphologic variants of the HMC in the axial plane. We also investigated sex-related differences in the distribution of the different HMC variants and their hemispheric combinations.

Materials and Methods

Subjects

As part of the continuing investigations of brain structures and functions of our institution, we obtained structural brain MR images from 257 young healthy right-handed subjects, all of whom provided written informed consent to participate in these studies. The subjects were recruited from hospital and institutional staff, student body, and the local community by either word of mouth or by advertisement. No subject had a history or MR imaging evidence of overt cerebral pathology as judged by a radiologist, and none had a history of alcohol or substance abuse or of any medical illness known to affect brain morphology. Additional exclusion criteria were history of head injury sufficient to have caused a coma; past or current history of central nervous system disease or a focal lesion incidentally discovered during this study; current or past history of a significant major medical disease; history of hypertension, diabetes, or current treatment with antihypertensives, insulin, or oral hypoglycemic; current pregnancy; significant use of drugs or stimulants in the 12 months before this study; and major mental illnesses as assessed by using the Structured Clinical Interview for DSM-III-R—Patient Version (SCID-P).²¹

The inclusion criteria were subjects who were strongly right-handed and between 22 and 35 years of age. The former inclusion criteria were implemented as part of the experimental design to exclude, as an experimental variable, the known relationship between handedness and the laterality of certain cerebral structures.²² Although this design implies that the potentially important relationship between degree of handedness and morphologic variants was not studied, we wished to study initially potential differences in a sex model in which we expected, on the basis of reports in literature, to observe variations.

Handedness was assessed by asking which hand the subject used for writing and was subsequently confirmed and quantified in all subjects by using the Italian revised version of the Edinburgh Handedness Inventory,²³ adapted by Salmaso and Longoni.²⁴ The questionnaire was self-reported and consisted of 12 items covering several daily actions. Subjects were asked to indicate which hand they would use to perform each task. A laterality quotient (LQ) ranging from -100 to 100 was calculated for each subject. In accordance with previous studies,^{24,25} subjects who obtained an $LQ < 0$ were considered left-handers and were excluded.

The mean age of the 143 men was 23.1 years with an SD of 1.1 years. The mean age of the 114 women was 23.0 years with an SD of 0.6 years. The difference between the 2 groups with regard to age was not significant ($t = -0.823$ with 256 degrees of freedom, $P = .411$, 2-tailed t test).

Imaging

MR images were acquired by using a 1.5T Magnetom Vision MR imaging scanner (Siemens, Erlangen, Germany). Structural imaging of the entire brain volume was obtained with a 3D magnetization-prepared rapid acquisition of gradient echo (MPRAGE) T1-weighted

sequence. The TR was 9.7 ms, TE was 4 ms, the FOV was 256 mm, section thickness was 1 mm, and flip angle was 12° . All images were obtained by using a matrix of 256×256 voxels and the in-plane voxel size of 1×1 mm. Structural data were transferred by using a digital format to a workstation equipped with an image-processing software (Brain Voyager 4.9; Brain Innovation, Maastricht, the Netherlands).

The entire scanned volume of each brain was transformed into Talairach space²⁶ in 2 steps: 1) translation and rotation of the cerebrum into the anterior/posterior commissure (ACPC) plane, and 2) identification of the borders of the cerebrum.

The software permitted the multiplanar reformatting of the 3D scanning volume and navigation within the brain by using navigation bars while allowing the simultaneous visualization of a selected point on the 3 spatial planes, thus permitting the extraction of 3D Talairach coordinates (x, y, z) for each selected voxel.

Morphologic Evaluation of the HMC

Before the morphologic evaluation of the HMC, all images were coded so that the operators were blinded to subjects' identities and sex. Hemispheres were randomly flipped so that the readers were also blinded for this characteristic. The operators first identified the precentral gyrus by using 2 methods: 1) recognizing the relationship between the foot of the precentral gyrus and the posterior aspect of the pars opercularis of the inferior frontal gyrus on the low hemispheric convexity,¹² and 2) identifying the typical course of the superior frontal and precentral sulci.¹⁰ The HMC was then localized by using standardized mean Talairach coordinates derived from a review of previously published articles,²⁷⁻³¹ which focused on the functional and anatomic localization of the HMC: $x = \pm 34$, $y = -29$, $z = 50$. After positioning the z -axis 50 Talairach mm above the ACPC line, we performed a visual morphologic classification of the HMC for the right and left hemispheres. If the resulting morphologic features of the HMC were not well defined, the positioning of the z -axis was varied by ± 2 Talairach mm to obtain a more-defined shape. The readers not only considered the previously described inverted omega and epsilon shapes¹⁷ but were also permitted to describe aberrant morphologic variants. To classify the variability observed in the epsilon form, we used an arbitrary method of visually separating the hand knob into 3 equal parts: lateral, central, and medial. Depending on the position of the third fissure, which segments the knob and modifies its appearance from an omega to an epsilon in the lateral, central, or medial part of the hand knob, we defined the variants as "medially asymmetric epsilon," "epsilon," and "laterally asymmetric epsilon," respectively (Fig 1). The height of the knob must be greater than the thickness of the precentral gyrus measured at the base of the knob to distinguish an "omega" from a "null." If the height was smaller than the thickness, the HMC was classified as "null."

Evaluation of Inter-Reader Variability

Two different expert neuroradiologists then independently evaluated the MR imaging studies of all the subjects, and interobserver reliability was evaluated by using the Kendall W test, which expresses the degree of association between 3 or more variables.

Statistical Analysis

An age difference between men and women was evaluated with a 2-tailed t test. The frequencies and percentages of the different morphologic variants of the HMC were calculated for right, left, and both hemispheres for all the 257 subjects, men only, and women only. Statistically significant differences in the frequencies of the different

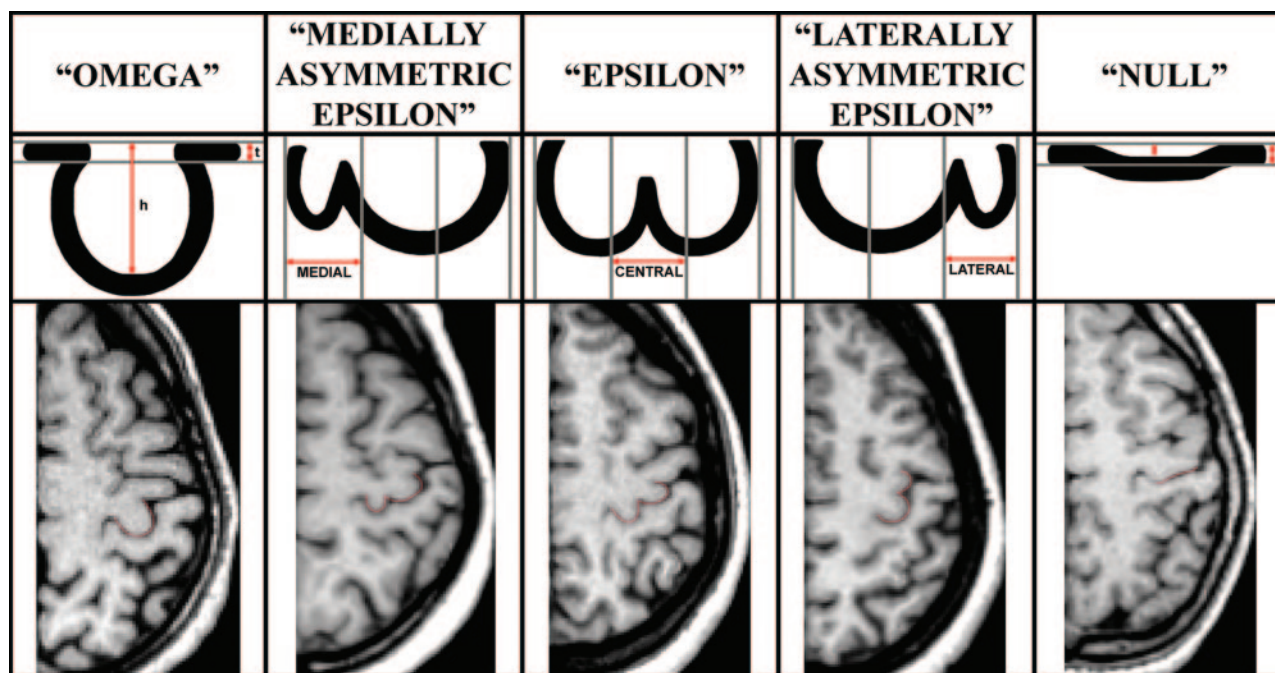


Fig 1. Schematic representation of the criteria used for morphologic classification and corresponding MR image of a typical example. The position of the third fissure, which segments the knob, modifying its appearance from an omega to an epsilon in the lateral, central, or medial part of the hand knob indicates a medially asymmetric epsilon, epsilon, and laterally asymmetric epsilon, respectively. To distinguish an omega from a null, the height of the knob must be greater than the thickness of the precentral gyrus measured at the base of the knob. If the height is smaller than the thickness, the HMC is classified as null. Multiplanar reformatted MR imaging axial sections were obtained from left hemispheres 50 ± 2 mm above the Talairach ACPC plane. The red area in the MR images highlights the morphologic variant.

morphologic variants of the HMC were assessed by using the χ^2 test. This comparison was performed treating the 3 variants of epsilon as a single group and then by separating the 3 variants. If a statistically significant difference was observed, then each morphologic variant was compared with all other morphologic variants by using the χ^2 test. A 5-by-5 table correlating the morphologic variants of the HMC between the 2 hemispheres was constructed. A subject was considered as concordant when the 2 hemispheres had the same morphologic variant or discordant when the 2 variants differed. The concordance of the morphologic variants between the 2 hemispheres for each sex was tested with the kappa test. All statistical calculations were performed with SPSS (Version 11.5 for Windows, SPSS, Chicago, Ill) and Medcalc (MedCalc Software, Mariakerke, Belgium). A $P < .01$ was considered statistically significant.

Results

Morphologic Variants of the HMC

The resulting morphologic features of the HMC were not well defined, requiring the repositioning of the z-axis by ± 2 Talairach mm in 42 (16.3%) cases. This variability was analogous to that observed in our routine practice and was not considered significant.

The 2 neuroradiologists described the shape of the HMC in the axial plane for all 514 hemispheres. The 3 new morphologic variants of HMC (laterally asymmetric epsilon, medially asymmetric epsilon, and null), other than the classic variants, were observed in both hemispheres for both sexes (Fig 1). Overall frequencies and percentages are reported in Table 1 and indicated that the most frequent morphologic variant of the HMC was the omega, followed by the epsilon, the laterally asymmetric epsilon, and the medially asymmetric epsilon; the null variant was the least frequent.

Frequencies of the Morphologic Variants

The frequencies and the percentage distribution of the 5 different HMC morphologic variants are reported for each hemisphere and sex in Table 1. The frequencies and the percentage distribution of the different combinations of the 5 morphologic variants of the HMC in the 2 hemispheres are reported in Table 2 and illustrated in Fig 2.

Sex Differences Between Hemispheres

A statistically significant difference between the 2 hemispheres was not observed overall (Table 1). When considering the 3 HMC morphologic variants of epsilon as a single group, we did not observe a statistically significant difference for sex, whereas we observed a statistically significant difference when considering the 3 epsilon variants as separate groups ($\chi^2 = 13.675$ with 4 df , $P = .008$). Comparison of each morphologic variant with all the other variants for sex indicated that the frequency of epsilon in men was twice that in women ($\chi^2 = 7.933$ with 1 df , $P = .005$).

Table 2 shows the concordance of the morphologic variants for the 2 hemispheres for men and women. Statistical analysis indicated that the concordance for morphologic variants between hemispheres was significant for women ($z = 3.03$, $P < .01$) but not for men ($z = 2.09$, not significant).

Inter-Reader Variability

The evaluation performed to estimate the interobserver reliability yielded a $W = 0.98$ ($P = .017$). These results indicated that the classification is highly repeatable. Most of the errors made by the 2 independent readers were between omega-null and between asymmetric epsilons-epsilon morphologic variants.

Table 1: HMC morphologic variants by gender

	Omega	Medially Asymmetric Epsilon	Epsilon	Laterally Asymmetric Epsilon	Null	Total
	No. (%)	No. (%)	No. (%)	No. (%)	No. (%)	No.
Overall						
Left hemisphere	201 (78.2)	7 (2.7)	31 (12.1)	14 (5.4)	4 (1.6)	257
Right hemisphere	201 (78.2)	8 (3.1)	21 (8.2)	22 (8.6)	5 (1.9)	257
Total	402 (78.2)	15 (2.9)	52 (10.1)	36 (7.0)	9 (1.8)	514
Men						
Left hemisphere	105 (73.4)	4 (2.8)	23 (16.1)	10 (7.0)	1 (0.7)	143
Right hemisphere	114 (79.7)	2 (1.4)	16 (11.2)	10 (7.0)	1 (0.7)	143
Total*	219 (76.6)	6 (2.1)	39 (13.6)	20 (7.0)	2 (0.7)	286
Women						
Left hemisphere	96 (84.2)	3 (2.6)	8 (7.0)	4 (3.5)	3 (2.6)	114
Right hemisphere	87 (76.3)	6 (5.3)	5 (4.4)	12 (10.5)	4 (3.5)	114
Total†	183 (80.3)	9 (3.9)	13 (5.7)	16 (7.0)	7 (3.1)	228

* $\chi^2 = 13.675$ with 4 df, $P = .008$.

† $\chi^2 = 7.933$ with 1 df, $P = .005$.

Table 2: Correlation of morphologic variants of the HMC for hemispheres in men and women

Left	Right					Total
	Omega	Medially Asymmetric Epsilon	Epsilon	Laterally Asymmetric Epsilon	Null	
Men*						
Omega	88 (61.5)	4 (2.8)	18 (12.6)	3 (2.1)	1 (0.7)	114 (79.7)
Medially asymmetric epsilon	2 (1.4)	0 (0.0)	0 (0.0)	0 (0.0)	0 (0.0)	2 (1.4)
Epsilon	8 (5.6)	0 (0.0)	4 (2.8)	4 (2.8)	0 (0.0)	16 (11.2)
Laterally asymmetric epsilon	7 (4.9)	0 (0.0)	1 (0.7)	2 (1.4)	0 (0.0)	10 (7.0)
Null	0 (0.0)	0 (0.0)	0 (0.0)	1 (0.7)	0 (0.0)	1 (0.7)
Total	105 (73.4)	4 (2.8)	23 (16.1)	10 (7.0)	1 (0.7)	143
Women†						
Omega	76 (66.7)	1 (0.9)	6 (5.3)	2 (1.8)	2 (1.8)	87 (76.5)
Medially asymmetric epsilon	5 (4.4)	1 (0.9)	0 (0.0)	0 (0.0)	0 (0.0)	6 (5.3)
Epsilon	3 (2.6)	0 (0.0)	1 (0.9)	1 (0.9)	0 (0.0)	5 (4.4)
Laterally asymmetric epsilon	9 (7.6)	1 (0.9)	1 (0.9)	1 (0.9)	0 (0.0)	12 (10.3)
Null	3 (2.6)	0 (0.0)	0 (0.0)	0 (0.0)	1 (0.9)	4 (3.5)
Total	96 (83.9)	3 (2.7)	8 (7.1)	4 (3.6)	3 (2.7)	114

Note:—Concordant hemispheres are in bold typeset.

* Kappa test: $z = 2.09$, $P < .05$ (not statistically significant).

† Kappa test: $z = 3.03$, $P < .01$.

Discussion

Other than the classic variants proposed by Yousry et al,¹⁷ we observed and classified 3 morphologic variants of HMC: laterally asymmetric epsilon, medially asymmetric epsilon, and null. Given the large sample group studied, these variants probably describe all the possible morphologic variants of the HMC and their combinations in the 2 hemispheres that radiologists and neuroscientists are likely to encounter in acquisitions on the axial plane.

The identification of the precentral gyrus on the cortical surface is the crucial initial step before the localization of other cortical regions or lesions of the brain. Therefore, a classification system that describes all the possible presenting forms of the HMC would be an aid in this step and would simplify the communication between neuroradiologists.

Several methods are currently used for recognizing and localizing the precentral gyrus on the basis of its relationship with other anatomic structures.^{10,12,15,32} The interindividual variability and discordance of the described anatomic landmarks³³ reduce the reliability of these methods for the identification of the precentral gyrus.³⁴

In addition to the use of morphologic methods for localizing cortical regions, fMRI with BOLD contrast technique has been used in the past few years to localize a region of the cerebral cortex on the basis of its activation during the execution of a specific task. The major drawbacks of this technique consist of a discrepancy between functional activations and their real anatomic positioning on the cerebral cortex³⁵ and in the limited availability of MR imaging systems and radiologists capable of performing fMRI and analysis. Furthermore, techniques other than or combined with structural imaging and fMRI have been used to localize the precentral gyrus and the HMC: direct electric cortical stimulation,² positron-emission tomography,¹¹ transcranial magnetic stimulation,^{30,36} and magnetoencephalography.³⁷ All these techniques localize the HMC in the same cortical region of the precentral gyrus but have major limits: They are time-consuming, invasive, or unavailable. Therefore, a practical method to easily recognize the cortical convolutions of the cerebral cortex by using anatomic landmarks remains fundamental in both healthy subjects and patients with brain lesions.

Yousry et al¹⁷ proposed a reliable method for localizing the

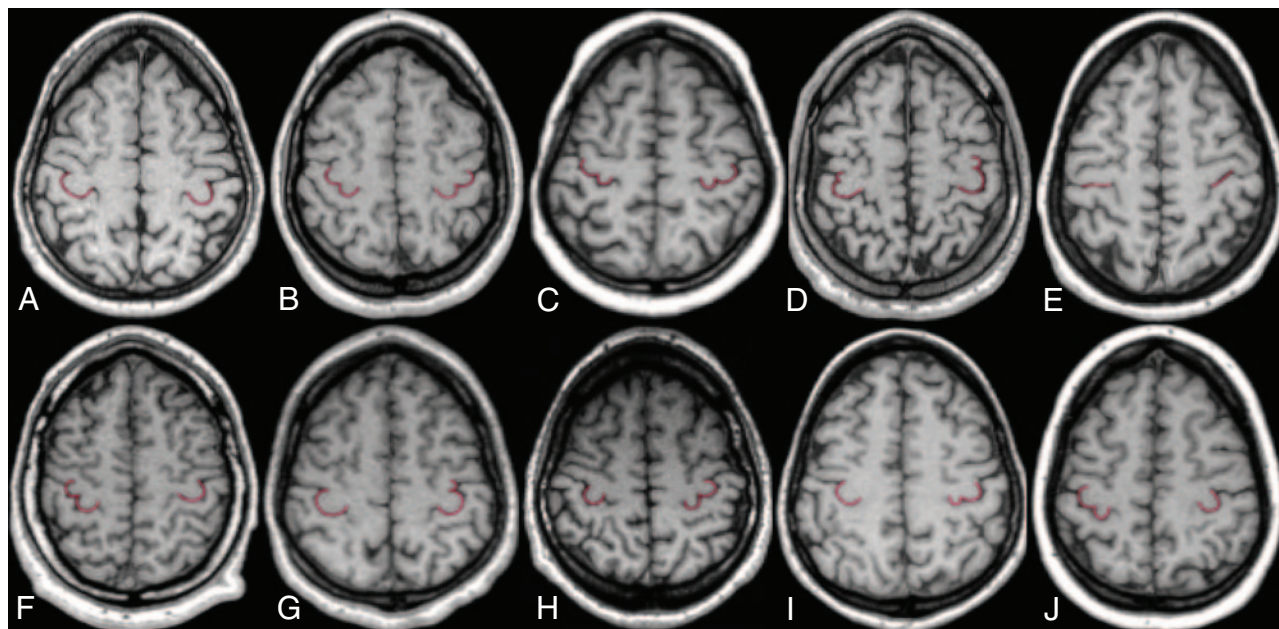


Fig 2. Multiplanar reformatted axial sections obtained 50 ± 2 mm above the Talairach anterior AC-PC plane. Images are shown using the right-left radiologic convention. The following are representative examples of the different combinations of HMC morphologic variants (red highlight) in the 2 hemispheres: *A*, Omega-omega. *B*, Epsilon-epsilon. *C*, Medially asymmetric epsilon-medially asymmetric epsilon. *D*, Laterally asymmetric epsilon-laterally asymmetric epsilon. *E*, Null-null. *F*, Epsilon-omega. *G*, Omega-laterally asymmetric epsilon. *H*, Omega-epsilon. *I*, Omega-medially asymmetric epsilon. *J*, Medially asymmetric epsilon-omega. The first 5 indicate concordant combinations, and the latter 5, the most common discordant combinations.

precentral gyrus based on the morphology of the HMC on the axial plane by using MR imaging. Due to the typical and constant inverted omega or epsilon shape, this anatomic landmark was the most sensitive for the identification of the precentral gyrus. This study was performed on a limited group of subjects and, therefore, given the tremendous interindividual variability of sulcation and gyrification of the cerebral cortex, probably did not include all the anatomic variants. To test this opinion and to complete the spectrum of morphologic variants of the HMC, the present study evaluated the morphology of the HMC in structural brain MR images of a larger group consisting of 257 right-handed men and women.

Adjusting the cerebral size of all subjects to fit in the Talairach space minimized operator-dependent variability in the identification of the HMC. Neuroscientists consider the Talairach atlas the standard reference for locating structural and functional areas.^{38,39} The 3D normalization approach described by Talairach and Tournoux²⁶ does not modify the morphology of sulcal and gyral arrangements^{40,41}; in particular, with this transformation, the central sulcus and the precentral gyrus present a minimal variability in position and morphology between individuals.^{27,42}

Only young subjects were included in this study to avoid any brain atrophy. In fact, clinical observations suggest that the normal aging process affects gyrification, with the brain appearing more atrophic with increasing age. Gyri become more sharply and steeply curved, while the sulci become more flattened with time.⁴³ In addition, cortical complexity and modification of sulcal topography of the frontal and parietal lobes, likely reflecting the ongoing process of myelination and synaptic remodeling, are known to continue until the second decade of life.⁴⁴ Therefore, subjects younger than 20 years of age were not enrolled in this study.

Statistical analysis of the frequencies of the different morpho-

logic variants for the 2 hemispheres did not yield a statistically significant difference. Differences were observed in the frequencies of the different morphologies between men and women. In particular, men had a statistically significant higher frequency of epsilon variant compared with women. However, when considering the 3 morphologic variants of epsilon (laterally asymmetric epsilon, epsilon, and medially symmetric epsilon) as a single group, we did not observe a statistically significant sex difference. The concordance for morphologic variants between hemispheres in men was not significant, indicating a higher interhemispheric asymmetry compared with that in women.

Sex-differences in the cortical arrangement have already been reported and correlate to a greater gyrification and cortical complexity in frontal and parietal regions in women than in men.¹⁸ If we consider the epsilon as the most complex morphologic variant of the HMC, due to its more complex underlying cortical anatomy, then the results of our study do not confirm those previously reported in literature. This discrepancy could be related to the use of 2D sequences in this study instead of the 3D reconstructions used by Luders et al.¹⁸

Differences in brain asymmetry between men and women have been demonstrated, indicating that the male brain is more asymmetric than the female brain.⁴⁵ Differences in the degree of structural asymmetry have been reported in cortical regions such as the planum temporale, the parietal lobe, and the posterior end of the Sylvian fissure.⁴⁶ Our results are in agreement with these findings.

The main limitation of this study was that the morphology of the HMC was evaluated on the axial plane, but this scanning plane is the most used by clinicians and neuroscientists and the one in which they have the most experience.

In this study, we included only right-handed subjects in view of the fact that handedness is known to influence the morphometry of the HMC, but an influence on morphology,

to our knowledge, has not been reported. Interhemispheric differences of the HMC correlated with handedness have been described in terms of asymmetry of the depth of the central sulcus, which in right-handers is higher in the left hemisphere than in the right.^{19,20} Functional imaging studies in humans have indicated that the knob is larger and more active in the hemisphere contralateral to the subject's preferred hand, which, in most cases, is the right hand.^{20,47}

Although we did not investigate correlations between morphologies and handedness, whether morphologic variants of the HMC and their interhemispheric combinations could reflect functional differences in hand motor behavior is an important question. Differences in morphology, in fact, can result in differences among some anatomic properties of the cortex, such as neuronal attenuation and connections, which, in turn, are known to correlate with differences in human behavior.⁴⁸ We therefore consider the possibility of a correlation between the anatomic variants of the HMC and differences in handedness. The validation of this hypothesis requires further study correlating HMC variants and behavioral data.

Conclusions

Five possible morphologic variants of the HMC in the axial plane and their different distributions in the brains of men and women were described. The new classification will be helpful for clinicians and neuroscientists in the routine localization of the central region of the brain.

Acknowledgment

We thank P.M. Rossini for his helpful comments concerning specific aspects of the interpretation of results.

References

1. Foerster O. *Motorische Felder und Bahnen*. In: Bumse H, Foerster O, eds. *Handbuch der Neurologie*. Berlin, Germany: Springer-Verlag; 1936:1–37
2. Penfield W, Boldrey E. Somatic motor and sensory representation in the cerebral cortex of man as studied by electrical stimulation. *Brain* 1937;60:389–443
3. Penfield W, Rasmussen T. *The cerebral cortex of man*. New York: McMillan; 1950
4. Hlustik P, Solodkin A, Gullapalli RP, et al. Somatotopy in human primary motor and somatosensory hand representations revisited. *Cereb Cortex* 2001;11:312–21
5. Hanakawa T, Parikh S, Bruno MK, et al. Finger and face representation in the ipsilateral pre-central motor areas in humans. *J Neurophysiol* 2005;93:2950–08
6. Cunningham DJ. *Contributions to the Surface Anatomy of the Cerebral Hemispheres*. Dublin, Ireland: Academy House; 1892
7. Dejerine J. *Anatomie des Centres Nerveux*. Vol 1. Paris, France: Rueff; 1895
8. Testut L. *Traite d'Anatomie Humaine*. Paris, France: Octave Doin et Fils; 1911
9. Ono M, Kubik S, Abernathy CD. *Atlas of the Cerebral Sulci*. New York: Thieme; 1990
10. Kido DK, LeMay M, Levinson AW, et al. Computed tomographic localization of the precentral gyrus. *Radiology* 1980;135:373–77
11. Rumeau C, Tzourio N, Murayama N, et al. Location of hand function in the sensorimotor cortex: MR and functional correlation. *AJNR Am J Neuroradiol* 1994;15:567–72
12. Naidich TP, Valavanis AG, Kubik S. Anatomic relationships along the low-middle convexity. Part I. Normal specimens and magnetic resonance imaging. *Neurosurgery* 1995;36:517–32
13. Salamon G, Martini P, Ternier F, et al. Topographical study of supratentorial brain tumors. *J Neuroradiol* 1991;18:123–40
14. Talairach J, Tournoux P. *Referentially oriented cerebral MRI anatomy*. New York: Thieme; 1993
15. Naidich TP, Brightbill TC. The pars marginalis: Part I: A 'bracket' sign for the central sulcus in axial plane CT and MRI. *Int J Neuroradiol* 1996;2:3–19
16. Puce A, Constable RT, Luby ML, et al. Functional magnetic resonance imaging of sensory and motor cortex: comparison with electrophysiological localization. *J Neurosurg* 1995;83:262–70

17. Yousry TA, Schmid UD, Alkadhi H, et al. Localization of the hand motor area to a knob on the precentral gyrus: a new landmark. *Brain* 1997;120:141–57
18. Luders E, Narr KL, Thompson PM, et al. Gender differences in cortical complexity. *Nat Neurosci* 2004;7:799–800
19. Zilles K, Schleicher A, Langemann C, et al. Quantitative analysis of sulci in the human cerebral cortex: development, regional heterogeneity, gender difference, asymmetry, intersubject variability and cortical architecture. *Hum Brain Mapp* 1997;5:218–21
20. Hopkins WD, Pilcher DL. Neuroanatomical localization of the hand motor area with magnetic resonance imaging: the left hemisphere is larger in great apes. *Behav Neurosci* 2001;115:1159–64
21. Spitzer RL, Williams JBW, Gibbon M, et al. *Structured Clinical Interview for DSM-III-R—Patient Edition (SCID-P) Version 1.0*. Washington, DC: American Psychiatric Press; 1990.
22. Barta P, Dazzan P. Hemispheric surface area: sex, laterality and age effects. *Cereb Cortex* 2003;13:364–70
23. Oldfield RC. The assessment and analysis of handedness: the Edinburgh inventory. *Neuropsychologia* 1971;9:97–113
24. Salmasso D, Longoni AM. Problems in the assessment of hand preference. *Cortex* 1985;21:533–49
25. Pia Viggiano M, Borelli P, Vannucci M, et al. Hand preference in Italian students. *Laterality* 2001;6:283–86
26. Talairach J, Tournoux P. *Co-Planar Stereotaxic Atlas of the Human Brain*. New York: Thieme; 1988
27. Sastre-Janer FA, Regis J, Belin P, et al. Three-dimensional reconstruction of the human central sulcus reveals a morphologic correlate of the hand area. *Cereb Cortex* 1998;8:641–47
28. Carey LM, Abbott DF, Egan GF, et al. The functional neuroanatomy and long-term reproducibility of brain activation associated with a simple finger tapping task in older healthy volunteers: a serial PET study. *Neuroimage* 2000;11:124–44
29. Beisteiner R, Windischberger C, Lanzenberger R, et al. Finger somatotopy in human motor cortex. *Neuroimage* 2001;13:1016–26
30. Lotze M, Kaethner RJ, Erb M, et al. Comparison of representational maps using functional magnetic resonance imaging and transcranial magnetic stimulation. *J Clin Neuropsychol* 2003;14:306–12
31. Agnew JA, Zeffiro TA, Edena GF. Left hemisphere specialization for the control of voluntary movement rate. *Neuroimage* 2004;22:289–303
32. Ebeling U, Steinmetz H, Huang YX, et al. Topography and identification of the inferior precentral sulcus in MR imaging. *AJR Am J Roentgenol* 1989;153:1051–56
33. Steinmetz H, Furst G, Freund HJ. Variation of perisylvian and calcarine anatomic landmarks within stereotaxic proportional coordinates. *AJNR Am J Neuroradiol* 1990;11:1123–30
34. Sobel DF, Gallen CC, Schwartz BJ, et al. Locating the central sulcus: comparison of MR anatomic and magnetoencephalographic functional methods. *AJNR Am J Neuroradiol* 1993;14:915–25
35. Yousry TA, Schmid UD, Schmidt D, et al. The central sulcal vein: a landmark identifying the central sulcus by functional MRI. *J Neurosurg* 1996;85:608–17
36. Boroojerdi B, Foltys H, Krings T, et al. Localization of the motor hand area using transcranial magnetic stimulation and functional magnetic resonance imaging. *Clin Neurophysiol* 1999;110:699–704
37. Volkmann J, Schnitzler A, Witte OW, et al. Handedness and asymmetry of hand representation in human motor cortex. *J Neurophysiol* 1998;79:2149–54
38. Carmack PS, Spence J, Gunst RF, et al. Improved agreement between Talairach and MNI coordinate spaces in deep brain regions. *Neuroimage* 2004;22:367–71
39. Mayka MA, Colcos DM, Leurgans SE, et al. Three-dimensional locations and boundaries of motor and premotor cortices as defined by functional brain imaging: a meta-analysis. *Neuroimage* 2006;31:1453–74
40. Fischl B, Sereno MI, Tootell RBH, et al. High-resolution intersubject averaging and a coordinate system for the cortical surface. *Hum Brain Mapp* 1999;8:272–84
41. Roland PE, Geyer S, Amunts K, et al. Cytoarchitectural maps of the human brain in standard anatomical space. *Hum Brain Mapp* 1997;5:222–27
42. Rademacher J, Burgel U, Geyer S, et al. Variability and asymmetry in the human precentral motor system: a cytoarchitectonic and myeloarchitectonic brain mapping study. *Brain* 2001;124:2232–58
43. Magnotta VA, Andreasen NC, Schultz SK, et al. Quantitative in vivo measurement of gyrfication in the human brain: changes associated with aging. *Cereb Cortex* 1999;9:151–60
44. Blanton RE, Levitt JG, Thompson PM, et al. Mapping cortical asymmetry and complexity patterns in normal children. *Psychiatry Res* 2001;107:29–43
45. Toga AW, Thompson PM. Mapping brain asymmetry. *Nat Rev Neurosci* 2003;4:37–48
46. Jancke L, Schlaug G, Huang Y, et al. Asymmetry of the planum parietale. *Neuroreport* 1994;5:1161–63
47. Triggs WJ, Calvanio R, Levine M. Transcranial magnetic stimulation reveals a hemisphere asymmetry correlate of intermanual differences in motor performance. *Neuropsychologia* 1997;35:1355–63
48. Witelson SF, Beresh H, Kigar DL. Intelligence and brain size in 100 postmortem brains: sex, lateralization and age factors. *Brain* 2006;129:386–98